Vibrational Properties of Hard and Soft Spheres Are Unified at Jamming

Francesco Arceri[*] and Eric I. Corwin

Department of Physics, University of Oregon, Eugene, Oregon 97403, USA

The unconventional thermal properties of jammed amorphous solids are directly related to their density of vibrational states. While the vibrational spectrum of jammed soft sphere solids has been fully described, the vibrational spectrum of hard spheres, a model glass former often related to physical colloidal glasses, is still unknown due to the difficulty of treating the nonanalytic interaction potential. We bypass this difficulty using the recently described effective interaction potential for the free energy of thermal hard spheres. By minimizing this effective free energy, we mimic the rapid compression of hard spheres and produce typical configurations of the thermal system. We measure the resulting vibrational spectrum and characterize its evolution toward the jamming point where configurations of hard and soft spheres are trivially unified. For densities approaching jamming from below, we observe low-frequency modes which agree with those found in numerical simulations of jammed soft spheres. Our measurements of the vibrational structure demonstrate that the jamming universality extends away from jamming: hard sphere thermal systems below jamming exhibit the same vibrational spectra as thermal and athermal soft sphere systems above the transition.

Introduction.—Glasses and granular materials are unified by their expression of amorphous rigidity. Seen from the perspective of granular systems, described as soft sphere packings, jamming marks the onset of rigidity and occurs at zero pressure, when every particle becomes fully constrained but all contacts are just kissing [1]. By contrast in hard sphere glasses, considered as shadow systems for colloidal glasses [2], rigidity is achieved at the dynamical glass transition [3,4] and the jamming point is only reached at infinite pressure when all the particles are forced to come into enduring kissing contact with one another [5]. As such, the jamming point is a matching point for the two systems, where hard sphere glasses end and soft sphere rigid solids begin. Even though the configurations found in each limiting case must be valid configurations for the other, there is no *a priori* reason to expect that the properties of such configurations should bear any meaningful relation due to their very different origins and interactions. Although the criticality of jamming has been explored from both hard and soft sphere perspectives [6–8], whether the jamming point represents a smooth crossover between hard and soft spheres or a singular point is still an open question. In this work, we demonstrate that the vibrational properties of both hard and soft sphere systems approach the jamming transition point in the same manner and show no discontinuity between behavior below and above jamming. We use an effective potential to bring packings of hard spheres to their free energy minima, allowing us to quench toward jamming without the limitations of conventional thermal simulations and to directly measure the vibrational spectrum from the dynamical matrix.
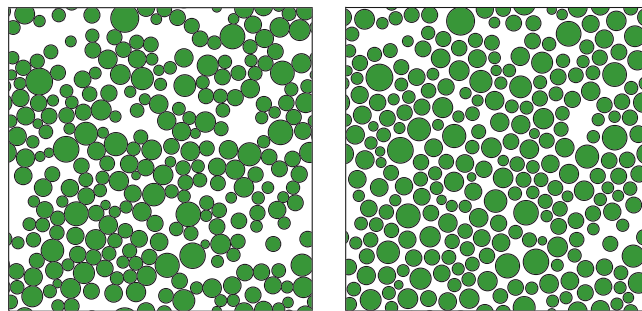
FIG. 1. Minimization of the effective logarithmic potential in $d = 2$ with packing fraction $\varphi = 0.55$. Left: packing after harmonic minimization. Right: final configuration of the same packing after the logarithmic potential minimization.

Amorphous solids exhibit vibrational properties very different from those predicted by Debye theory [9–11]. The replica mean field theory of glasses and jamming predicts the low-frequency scaling of the vibrational density of states (VDOS) to behave as $D(\omega) \sim \omega^2$ for systems in every spatial dimension [12–15]. This non-Debye scaling has been observed numerically in systems of soft spheres right above the jamming point [16] and is the result of an excess of vibrational modes within this low-frequency range. These excess modes are spatially extended but nonphononic and give rise to a peak in the heat capacity of glasses, often called the boson peak [17–19]. The VDOS associated with these modes is nearly flat for low frequencies ranging down to a crossover frequency ω^* below which it decays to zero [20]. At jamming, even an infinitesimal excitation

leads to an extended motion and the VDOS is flat until $\omega^* = 0$ [21].

In contrast to the mean field picture, as low-dimensional soft sphere systems are brought to densities above jamming, an additional class of modes appears as quasilocalized modes which are hybridized between system spanning phonons and local rearrangements [22]. These modes are believed to control the elastic response to externally applied shears [23,24] and are measured to follow a low-frequency scaling of $D_{\text{loc}}(\omega) \sim \omega^4$ [25–28]. Such a scaling result has been observed for a wide variety of disordered systems [29–31]. These quasilocalized modes do not appear in the mean field picture as they are exclusively a low-dimensional phenomenon [32].

Similar quasilocalized modes play a central role in the physics of real low-temperature glasses [33,34]. They are described as soft excitations that connect two local minima of the free energy, a scenario introduced by Phillips in the two-level tunneling model [35,36]. These modes can be derived from anharmonic effects which are directly related to the nonanalytic form of the hard sphere potential [34,37–39]. Anharmonic effects independently arise from perturbation theory of hard spheres near jamming [15,40], where the free energy has been found to be well approximated by a logarithmic effective pair potential [41] and higher order corrections to this behavior are unnecessary even at a finite distance to the jamming point [42]. The same effective interaction has also been shown in simulations of thermal hard spheres under very high pressure [43] for which an effective medium theory has been developed [44].

In the limit of high pressure thermal hard spheres, this effective logarithmic potential can be understood as deriving from entropic consideration. If the typical timescale between collisions is much smaller than the typical timescale for relaxational rearrangements, then the time average of the momenta exchanged between frequently colliding particles is inversely proportional to the gap h between those particles [43]. This coarse graining over time defines a network of effective forces between hard spheres with corresponding potential energy given by a sum of two-body logarithmic potentials of the form

$$V(h) = -k_B T \log(h). \tag{1}$$

Thermal hard spheres near jamming can thus be directly mapped to a collection of athermal particles interacting via the logarithmic effective potential.

While the mean field theory predicts the same vibrational properties for hard spheres below jamming and soft spheres above jamming, in low-dimensional systems the vibrational spectra could be very dissimilar due to the very different circumstances giving rise to quasilocalized modes. In this Letter, we present a protocol to produce stable glassy configurations based on the minimization of the effective
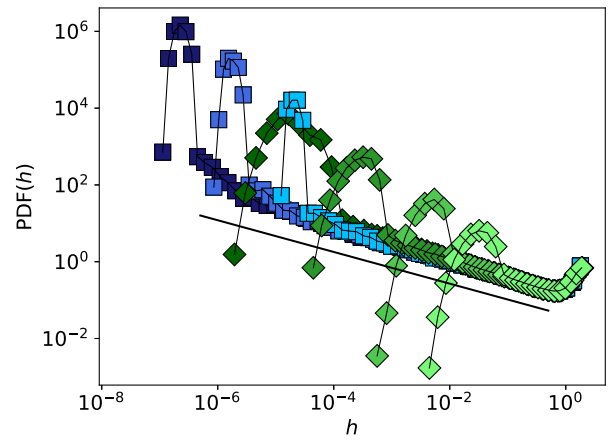
FIG. 2. Gap distribution of hard sphere packings in $d = 3$. The distance from jamming increases from left to right: data from decompressions (blue squares) $\Delta\varphi = 1.1 \times 10^{-7}, 1.3 \times 10^{-6}, 1.5 \times 10^{-5}$, data from compressions (green diamonds) $\Delta\varphi = 2.3 \times 10^{-5}, 2.1 \times 10^{-4}, 3 \times 10^{-3}, 2 \times 10^{-2}$. The distributions peak around the value of the typical nearest neighbor gap and then decay following a power-law scaling (black line) consistent with the mean field prediction $h^{-\gamma}$ with $\gamma = 0.41296\ldots$ [5]. Gaps are cutoff at $h = 1$ to avoid showing next nearest neighbor behavior.

free energy potential for a packing of athermal hard spheres. By measuring the evolution of the vibrational spectrum approaching jamming, we show that the spectrum of jammed solids is unified when crossing the transition between the hard and the soft sphere descriptions. This result demonstrates that mechanical and thermal properties of jammed solids arise purely from a geometric origin.

Numerical methods.—Hard sphere packings are produced using the pyCudaPacking package, developed by Corwin *et al.* [7,45]. The packing is a collection of N particles in $d = 2, 3$ spatial dimensions, with a log-normal distribution of particle sizes chosen to avoid crystallization. The packing is inside a box of unit volume with periodic boundary conditions and characterized by the packing fraction φ, the fraction of the box volume occupied by particles.

Starting from a packing fraction well below jamming we randomly distribute particles and minimize energy using a harmonic interaction potential (the same as used in the context of soft spheres [46]) to eliminate any overlap between particles. The logarithmic potential is then applied as a pair potential between particles separated by less than a cutoff gap distance. This cutoff is chosen to be twice the value of the position of the first peak of the gap distribution to allow for nearest neighbor interactions and exclude the nonphysical next nearest neighbor interactions. However, all the results reported herein are insensitive to this choice as long as the cutoff encompasses nearest neighbors; see the Supplemental Material [47]. We then minimize the potential using the FIRE (Fast Inertial Relaxation Engine) algorithm [48].

The result of the minimization of the logarithmic potential is depicted in Fig. 1. From an initial packing characterized by a broad distribution of nearest neighbor gaps, the system reaches a configuration where the nearest neighbor gaps are more uniform. This resulting packing is compatible with the time-averaged limit of a thermal hard sphere system, where collisions push particles as far as possible from their neighbors on average [43]. If φ is less than the jamming packing fraction φ_J, then no particles are in contact after the minimization and a void region can be found around each particle. We exploit this to creep up in density by inflating particles until saturating 10% of the minimum gap and then minimizing the effective potential for this new packing fraction. Repeating this procedure iteratively, we are able to push the system to a distance from jamming $\Delta\varphi = |\varphi_J - \varphi|$ of the order of 10^{-6}. To produce packings at densities significantly closer to jamming, we decompress critically jammed soft sphere configurations and then minimize the logarithmic potential [7]. By slightly decompressing these packings, we maintain the same spatial structure of the jammed systems, with a precise tuning of the distance from jamming $\Delta\varphi$.

Figure 2 shows the gap distribution from both compressions and decompressions exhibiting the same behavior. We find a power-law scaling of the gap distribution that is well described by the mean field scaling law $h^{-\gamma}$ [5] and has previously been measured for soft spheres precisely at jamming [7]. The systems created by decompression from jamming show a sharper peak for the nearest gaps than is found in systems created through compression, even when both systems are at nearly the same distance from the jamming transition. This reflects the underlying property that systems created from jammed soft spheres will maintain a memory of their kissing contacts, while those compressed from below have not yet chosen a single set of incipient contacts and thus have a broader distribution. Nevertheless, for every protocol, the distribution of nearest gaps tends to a delta function upon approach to the jamming point as the nearest neighbors become contacts.

Vibrational spectrum analysis.—In order to distinguish extended and localized modes, we compute the participation ratio (PR) of each mode, a measure of the fraction of particles that are participating in the motion governed by the mode. Given a mode at frequency ω with eigenvectors $\{\mathbf{u}_i(\omega)\}$, where $\mathbf{u}_i$ is the displacement vector for particle i, we define the PR as

$$\text{PR}(\omega) = \frac{1}{N_s} \frac{[\sum_i^{N_s} |\mathbf{u}_i(\omega)|^2]^2}{\sum_i^{N_s} |\mathbf{u}_i(\omega)|^4}, \tag{2}$$

where N_s is the number of stable particles, i.e., those with at least $z = d + 1$ force bearing neighbors [49]. A mode that corresponds to a totally extensive motion in which every particle participates equally will be characterized by
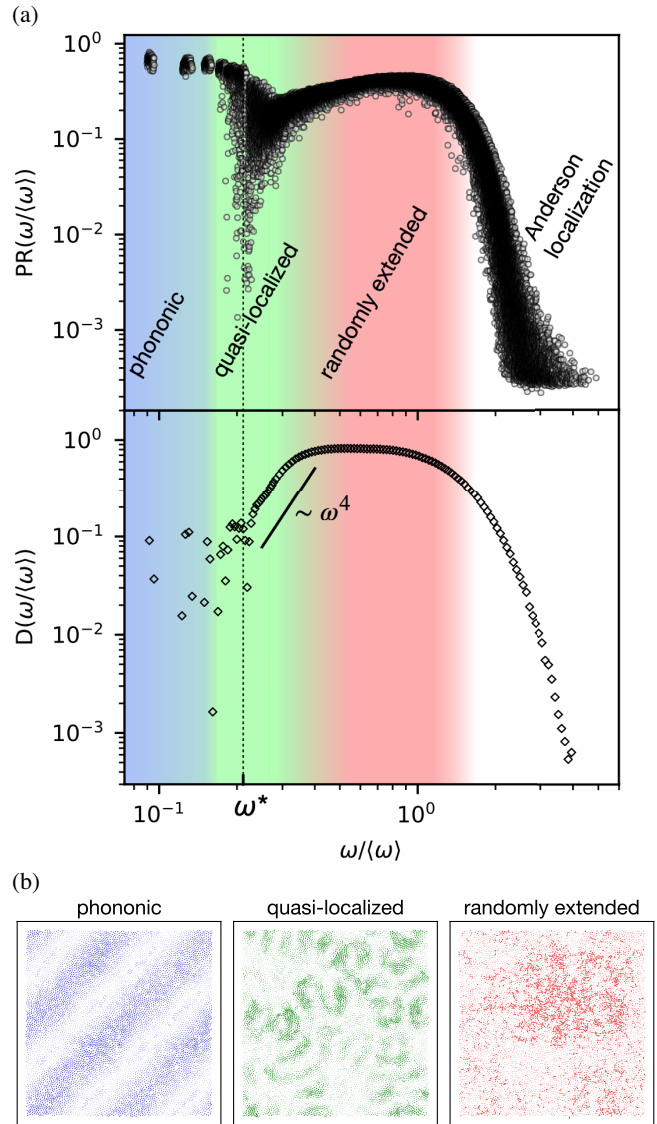
FIG. 3. (a) Participation ratio (PR) and vibrational density of states for a packing of $N = 8192$ particles in $d = 3$ at $\Delta\varphi = 3 \times 10^{-2}$. (b) Real space representation of the eigenvectors for a packing of $N = 8192$ particles in $d = 2$ with distance from jamming $\Delta\varphi = 3 \times 10^{-2}$. Left: phonon with characteristic plane wave modulation. Center: quasilocalized mode with localized excitations distributed over the whole system. Right: extended anomalous mode which correlates a large portion of the system with random excitations.

PR $= 1$, whereas a mode completely localized to a single particle will have PR $= 1/N_s$ [16,22].

The vibrational spectrum for both two- and three-dimensional packings produced by minimization of the logarithmic potential can be divided into four different ranges of frequency as illustrated in Fig. 3(a), ranging from lowest to highest frequency: (1) at lowest frequencies, the modes separate into discrete phonon bands with PR $\simeq 2/3$ as expected for plane waves [22,28] (blue region). (2) For frequencies close to ω^*, we find quasilocalized modes
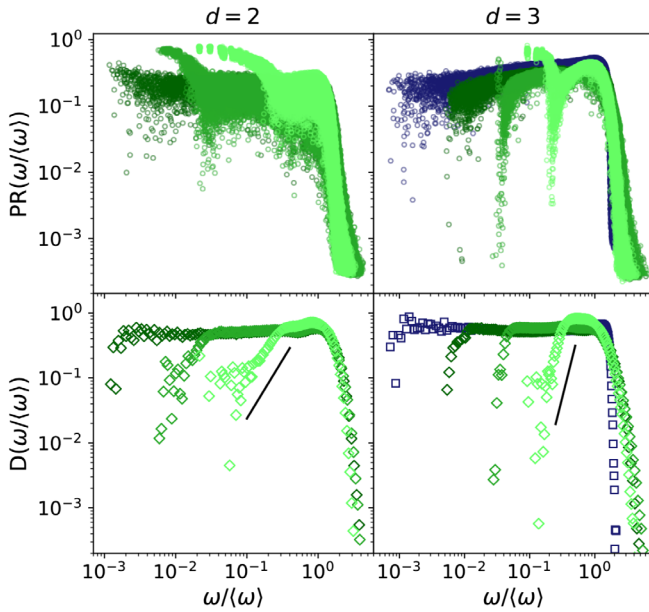
FIG. 4. Evolution of participation ratio (PR) and vibrational density of states along the compression as a function of $\Delta\varphi$ in $d = 2$ (left) and $d = 3$ (right). Data from compressions are shown in green and that from decompressions in $d = 3$ in blue. Each scatter plot of PR shows data from 10 samples while the density of state curves are averaged over the same number of samples. The distance from jamming increases from left to right. In $d = 3$ $\Delta\varphi = 1.1 \times 10^{-7}$, $\Delta\varphi = 2.3 \times 10^{-5}, 5 \times 10^{-4}, 3 \times 10^{-2}$. In $d = 2$ $\Delta\varphi = 2.7 \times 10^{-6}, 3 \times 10^{-4}, 3 \times 10^{-2}$. The low-frequency decay of the density of states in $d = 2$ follows ω^2 for every value of $\Delta\varphi$, while in $d = 3$ it follows ω^4 sufficiently far from jamming.

which show a splitting in the PR and a power-law decay in the density of states (green region). (3) For higher frequencies, modes become increasingly delocalized as indicated by a very high PR. This region corresponds to extended anomalous modes as evidenced by a nearly flat density of states (red region). (4) At highest frequencies, modes are strongly localized as a result of Anderson localization in a random medium and have a density of states that decays rapidly with increasing frequency [26].

We analyze the diverse nature of the vibrational modes by looking at the real space representation of their eigenvectors shown in Fig. 3(b). Phonons (left) have a typical plane wave modulation which spans the system. Quasilocalized modes (center), with frequencies near ω^*, present a number of localized distortions and vortices hybridized with those phonons at nearby frequencies. Extended anomalous modes (right) contain random seeming excitations spread throughout the entire system.

As shown in Fig. 4, systems in two and three dimensions differ significantly within the quasilocalized frequency range as evidenced both in the PR and the VDOS. Three-dimensional systems have a greater fraction of modes with strong localization than in two-dimensional systems. This difference manifests in the functional form of
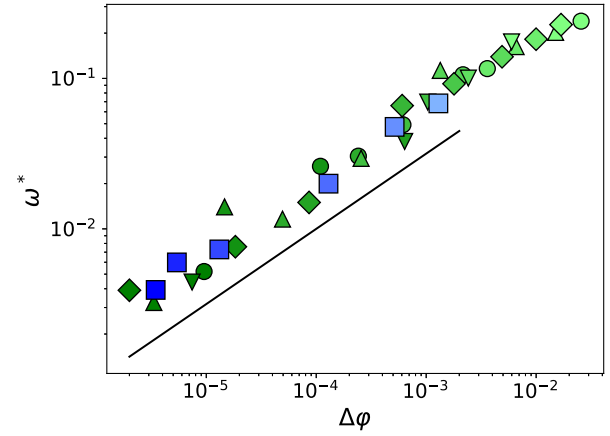
FIG. 5. Scaling of ω^* as a function of $\Delta\varphi$ for different system sizes from decompressions (blue squares $N = 4096$) and compressions (green circles $N = 1024$, upward triangles $N = 2048$, downward triangles $N = 4096$, diamonds $N = 8192$). Data are consistent with the critical scaling $\omega^* \sim \Delta\varphi^{1/2}$ observed for soft spheres.

the decay of the VDOS. For $d = 3$, the density of quasilocalized modes dominates over that of extended modes as evidenced by a decay that follows the ω^4 law. For $d = 2$ instead, a continuous crossover between phonons and extended modes dominates this region of the spectrum with a decay of the density that goes as ω^2. These results for hard sphere systems below jamming agree with previous observations for soft spheres above the jamming threshold [22].

Criticality near jamming.—Figure 4 shows the evolution of the density of states and the participation ratio for systems in both $d = 2$ and $d = 3$ at a broad range of distances from jamming. As jamming is approached, quasilocalized modes move toward lower frequencies and hybridize with the existing phonons as local excitations get softer [29]. For a range of densities sufficiently far from jamming, quasilocalized modes coexist with phonons. For $\Delta\varphi \lesssim 10^{-4}$, extended modes dominate the vibrational spectrum. Localized excitations disappear due to the increasing stability of the packing from the compression, a property which translates into a reduction of the number of soft spots from which localized excitations originate [29]. We observe that for $\Delta\varphi \lesssim 10^{-5}$ localized distortions are suppressed for both spatial dimensions as the extended mode plateau reaches down toward $\omega = 0$. We observe that in $d = 3$ the low-frequency scaling of the VDOS deviates from the ω^4 law while in $d = 2$ the ω^2 scaling holds for every step of the compression.

We measure ω^* as the frequency of the last extended mode above a cutoff in participation ratio, $PR_c = 8 \times 10^{-2}$. As shown in the Supplemental Material [47], the results are insensitive to the choice of PR_c for $8 \times 10^{-2} < PR_c < 2 \times 10^{-1}$. The relationship of ω^* on $\Delta\varphi$ is reported in Fig. 5. The resulting scaling law is consistent with that

already found in the jamming critical region for harmonic soft spheres [6].

Conclusions.—By minimizing the logarithmic effective potential, we are able to track the structural features from which the mechanical properties of hard sphere glasses originate, both below jamming and at the transition. We have exploited the analytic effective potential to implement a deterministic minimization algorithm and to compute the vibrational properties of hard sphere glasses, something which previously was accessible only from the velocity autocorrelation function in thermal simulations [34]. The vibrational modes found below and at jamming using this effective potential quantitatively agree with those observed in soft sphere systems above the transition. Thus, we have demonstrated that granular systems and the shadow systems of colloidal glasses have the same vibrational properties at jamming and approaching the transition. Further, the scaling of ω^* confirms that the jamming criticality is universal from both the hard and the soft sides of the transition: thermal hard spheres under very high pressure (or their athermal mapping in this case) have the same criticality as a packing of harmonic soft spheres brought close to zero pressure.

This work suggests several paths forward for studying hard sphere glassy systems using the tools developed for athermal soft sphere systems. First, it would be useful to apply these techniques to develop a more detailed characterization of the size distribution of soft spots in higher dimension, for which existing methods in identifying quasilocalized modes are not sufficient. Further development of real-space characterizations of these modes will allow for investigations of spatial correlations of quasilocalized modes and how the associated length scale evolves toward jamming. Another future direction will be to minimize the logarithmic potential in a previously equilibrated hard sphere glass [8]. By doing so, it will be possible to isolate structural features from thermal noise and study mechanical and rheological properties directly related to the real space glassy structure.

*Corresponding author.
farceri@uoregon.edu

[1] C. S. O'Hern, S. A. Langer, A. J. Liu, and S. R. Nagel, Random Packings of Frictionless Particles, Phys. Rev. Lett. **88**, 075507 (2002).

[2] K. Chen, M. L. Manning, P. J. Yunker, W. G. Ellenbroek, Z. Zhang, A. J. Liu, and A. G. Yodh, Measurement of Correlations between Low-Frequency Vibrational Modes and Particle Rearrangements in Quasi-Two-Dimensional Colloidal Glasses, Phys. Rev. Lett. **107**, 108301 (2011).

[3] C. A. Angell, Perspective on the glass transition, J. Phys. Chem. Solids **49**, 863 (1988).

[4] L. Berthier and G. Biroli, Theoretical perspective on the glass transition and amorphous materials, Rev. Mod. Phys. **83**, 587 (2011).

[5] P. Charbonneau, J. Kurchan, G. Parisi, P. Urbani, and F. Zamponi, Glass and jamming transitions: From exact results to finite-dimensional descriptions, Annu. Rev. Condens. Matter Phys. **8**, 265 (2017).

[6] N. Xu, M. Wyart, A. J. Liu, and S. R. Nagel, Excess Vibrational Modes and the Boson Peak in Model Glasses, Phys. Rev. Lett. **98**, 175502 (2007).

[7] P. Charbonneau, E. I. Corwin, G. Parisi, and F. Zamponi, Jamming Criticality Revealed by Removing Localized Buckling Excitations, Phys. Rev. Lett. **114**, 125504 (2015).

[8] L. Berthier, P. Charbonneau, Y. Jin, G. Parisi, B. Seoane, and F. Zamponi, Growing timescales and lengthscales characterizing vibrations of amorphous solids, Proc. Natl. Acad. Sci. U.S.A. **113**, 8397 (2016).

[9] P. Debye, Zur Theorie der spezifischen Wrmen, Ann. Phys. (Berlin) **344**, 789 (1912).

[10] R. C. Zeller and R. O. Pohl, Thermal conductivity and specific heat of noncrystalline solids, Phys. Rev. B **4**, 2029 (1971).

[11] U. Buchenau, A. Wischnewski, M. Ohl, and E. Fabiani, Neutron scattering evidence on the nature of the boson peak, J. Phys. Condens. Matter **19**, 205106 (2007).

[12] G. Parisi and F. Zamponi, Mean-field theory of hard sphere glasses and jamming, Rev. Mod. Phys. **82**, 789 (2010).

[13] M. Wyart, Scaling of phononic transport with connectivity in amorphous solids, Europhys. Lett. **89**, 64001 (2010).

[14] H. Jacquin, L. Berthier, and F. Zamponi, Microscopic Mean-Field Theory of the Jamming Transition, Phys. Rev. Lett. **106**, 135702 (2011).

[15] S. Franz, G. Parisi, P. Urbani, and F. Zamponi, Universal spectrum of normal modes in low-temperature glasses, Proc. Natl. Acad. Sci. U.S.A. **112**, 14539 (2015).

[16] P. Charbonneau, E. I. Corwin, G. Parisi, A. Poncet, and F. Zamponi, Universal Non-Debye Scaling in the Density of States of Amorphous Solids, Phys. Rev. Lett. **117**, 045503 (2016).

[17] P. W. Anderson, B. I. Halperin, and C. M. Varma, Anomalous low-temperature thermal properties of glasses and spin glasses, Philos. Mag. **25**, 1 (1972).

[18] T. Nakayama, Boson peak and terahertz frequency dynamics of vitreous silica, Rep. Prog. Phys. **65**, 1195 (2002).

[19] K. Chen, W. G. Ellenbroek, Z. Zhang, D. T. N. Chen, P. J. Yunker, S. Henkes, C. Brito, O. Dauchot, W. van Saarloos, A. J. Liu, and A. G. Yodh, Low-Frequency Vibrations of Soft Colloidal Glasses, Phys. Rev. Lett. **105**, 025501 (2010).

[20] C. S. OHern, L. E. Silbert, A. J. Liu, and S. R. Nagel, Jamming at zero temperature and zero applied stress: The epitome of disorder, Phys. Rev. E **68**, 011306 (2003).

[21] L. Yan, E. DeGiuli, and M. Wyart, On variational arguments for vibrational modes near jamming, Europhys. Lett. **114**, 26003 (2016).

[22] H. Mizuno, H. Shiba, and A. Ikeda, Continuum limit of the vibrational properties of amorphous solids, Proc. Natl. Acad. Sci. U.S.A. **114,** E9767 (2017).

[23] C. E. Maloney and A. Lemaitre, Amorphous systems in athermal, quasistatic shear, Phys. Rev. E **74,** 016118 (2006).

[24] M. L. Manning and A. J. Liu, Vibrational Modes Identify Soft Spots in a Sheared Disordered Packing, Phys. Rev. Lett. **107,** 108302 (2011).

[25] V. Mazzacurati, G. Ruocco, and M. Sampoli, Low-frequency atomic motion in a model glass, Europhys. Lett. **34,** 681 (1996).

[26] N. Xu, V. Vitelli, A. J. Liu, and S. R. Nagel, Anharmonic and quasi-localized vibrations in jammed solids–modes for mechanical failure, Europhys. Lett. **90,** 56001 (2010).

[27] E. Lerner, G. Dring, and E. Bouchbinder, Statistics and Properties of Low-Frequency Vibrational Modes in Structural Glasses, Phys. Rev. Lett. **117,** 035501 (2016).

[28] L. Wang, A. Ninarello, P. Guan, L. Berthier, G. Szamel, and E. Flenner, Low-frequency vibrational modes of stable glasses, Nat. Commun. **10,** 26 (2019).

[29] L. E. Silbert, A. J. Liu, and S. R. Nagel, Vibrations and Diverging Length Scales Near the Unjamming Transition, Phys. Rev. Lett. **95,** 098301 (2005).

[30] M. Baity-Jesi, V. Martin-Mayor, G. Parisi, and S. Perez-Gaviro, Soft Modes, Localization, and Two-Level Systems in Spin Glasses, Phys. Rev. Lett. **115,** 267205 (2015).

[31] A. Widmer-Cooper, H. Perry, P. Harrowell, and D. R. Reichman, Irreversible reorganization in a supercooled liquid originates from localized soft modes, Nat. Phys. **4,** 711 (2008).

[32] P. Morse, S. Wijtmans, M. van Deen, M. van Hecke, and M. L. Manning, Two classes of events in sheared particulate matter, Phys. Rev. Research **2,** 023179 (2020).

[33] E. Lerner, G. Dring, and M. Wyart, Low-energy non-linear excitations in sphere packings, Soft Matter **9,** 8252 (2013).

[34] A. Ikeda, L. Berthier, and G. Biroli, Dynamic criticality at the jamming transition, J. Chem. Phys. **138,** 12A507 (2013).

[35] W. A. Phillips, Tunneling states in amorphous solids, J. Low Temp. Phys. **7,** 351 (1972).

[36] Yu. M. Galperin, V. L. Gurevich, and D. A. Parshin, Theory of low-temperature thermal expansion of glasses, Phys. Rev. B **32,** 6873 (1985).

[37] V. G. Karpov and D. A. Parshin, The thermal conductivity of glasses at temperatures below the Debye temperature, Zh. Eksp. Teor. Fiz. **88,** 2212 (1985).

[38] U. Buchenau, Yu. M. Galperin, V. L. Gurevich, D. A. Parshin, M. A. Ramos, and H. R. Schober, Interaction of soft modes and sound waves in glasses, Phys. Rev. B **46,** 2798 (1992).

[39] V. L. Gurevich, D. A. Parshin, and H. R. Schober, Anharmonicity, vibrational instability, and the boson peak in glasses, Phys. Rev. B **67,** 094203 (2003).

[40] S. Franzand and G. Parisi, The simplest model of jamming, J. Phys. A **49,** 145001 (2016).

[41] A. Altieri, S. Franz, and G. Parisi, The jamming transition in high dimension: An analytical study of the TAP equations and the effective thermodynamic potential, J. Stat. Mech. (2016) 093301.

[42] A. Altieri, Higher-order corrections to the effective potential close to the jamming transition in the perceptron model, Phys. Rev. E **97,** 012103 (2018).

[43] C. Britoand and M. Wyart, Geometric interpretation of previtrification in hard sphere liquids, J. Chem. Phys. **131,** 024504 (2009).

[44] E. DeGiuli, E. Lerner, and M. Wyart, Theory of the jamming transition at finite temperature, J. Chem. Phys. **142,** 164503 (2015).

[45] P. K. Morse and E. I. Corwin, Geometric Signatures of Jamming in the Mechanical Vacuum, Phys. Rev. Lett. **112,** 115701 (2014).

[46] D. J. Durian, Foam Mechanics at the Bubble Scale, Phys. Rev. Lett. **75,** 4780 (1995).

[47] See Supplemental Material at http://link.aps.org/supplemental/10.1103/PhysRevLett.124.238002 for independence of the mode localization on the gap distance cutoff and insensitivity of ω^* on the participation ratio cutoff threshold.

[48] E. Bitzek, P. Koskinen, F. Ghler, M. Moseler, and P. Gumbsch, Structural Relaxation Made Simple, Phys. Rev. Lett. **97,** 170201 (2006).

[49] C. P. Goodrich, A. J. Liu, and S. R. Nagel, Finite-Size Scaling at the Jamming Transition, Phys. Rev. Lett. **109,** 095704 (2012).